

Numerical and theoretical modelling of low velocity impact on UHPC panels

Prabhat R. Prem^{*}, Mohit Verma^a, A. Ramachandra Murthy^a, J. Rajasankar^a and B.H. Bharatkumar^a

CSIR-Structural Engineering Research Centre, Chennai, 600 113, India

(Received August 5, 2016, Revised February 3, 2017, Accepted March 10, 2017)

Abstract. The paper presents the studies carried out on low velocity impact of Ultra high performance concrete (UHPC) panels of size $350 \times 350 \times 10 \text{ mm}^3$ and $350 \times 350 \times 15 \text{ mm}^3$. The panels are cast with 2 and 2.5% micro steel fibre and compared with UHPC without fiber. The panels are subjected to low velocity impact, by a drop-weight hemispherical impactor, at three different energy levels of 10, 15 and 20 J. The impact force obtained from the experiments are compared with numerically obtained results using finite element method, theoretically by energy balance approach and empirically by nonlinear multi-genetic programming. The predictions by these models are found to be in good coherence with the experimental results.

Keywords: ultra high performance concrete; low velocity impact; finite element; energy balance model; empirical relation

1. Introduction

There is growing need for advanced building materials for high-performance construction and retrofitting of existing structures. These materials should also be sustainable and durable. Ultra high performance concrete (UHPC) is one such advanced cementitious composite having very high compressive strength, tensile/flexural strength and durability characteristics (Schmidt and Fehling 2005, Wille *et al.* 2011, Maca *et al.* 2014). UHPC also shows enhanced strain hardening properties due to crack bridging of micro steel fibers with multiple cracking. This leads to quasi-ductile behavior, formation of new crack surfaces with numerous fiber pullout, increased fracture energy and toughness. These properties enable the application of UHPC for dam repair, bridge deck overlays, coupling beams in high rise building, specialized structures (Rokugo *et al.* 2009, Naaman *et al.* 2011, Schmidt 2012) and impact resistance (Sohel *et al.* 2003, Farnam *et al.* 2010, Mechtcherine *et al.* 2011). It is also very important to safeguard structures against extreme dynamic loads such as earthquakes, explosions, car or plane crash and to terrorist attacks. In this regard, UHPC is seen as one of the most promising candidates for absorbing energy against quasi-static and dynamic loading (Sovjak *et al.* 2015).

Recently extensive research has been carried out by authors on development of mix design (Prem *et al.* 2012, Ambily *et al.* 2015), methodology of curing (Prem *et al.* 2013, 2015a), determination of fracture properties (Murthy *et al.* 2013), repairing flexural members (Prem *et al.* 2015b, Prem and Murthy 2016) with UHPC. It was also demonstrated that UHPC can be successfully used as

precast and cast in situ members (Murthy *et al.* 2014). But it was found that the understanding of the impact resistance of UHPC is limited. Due to absence of standard guidelines for evaluating impact resistance of concrete, researchers have used different impact machines, specimen configurations, instrumentation and analysis schemes (Habel and Gauvreau 2008, Zhang *et al.* 2010, Farnam *et al.* 2010, Tai and Wang 2011, Yu *et al.* 2014). In other studies, Maca *et al.* (2014) studied the response of UHPC to deformable and non-deformable projectile impact by assessing the damage based on penetration depth, crater diameter and loss of mass. Yoo *et al.* (2015) reported studies on UHPC beams with different reinforcement ratio under impact loading. Xu *et al.* (2016) presented experimental results of 8 columns under explosions at different scaled distances. The results showed that UHPC specimens can effectively resist the overpressures and shock waves resulted from high explosives. In earlier studies on impact loading authors reported, impact behavior of steel polymeric hybrid fiber reinforced mortar and UHPC using instrumented drop weight impact machine. It is observed that the partial replacement of polymeric fiber with steel fiber, changes the failure mode of polymeric fiber from brittle to ductile and increases the energy absorption capacity. However, the improvement due to the steel fiber addition is relatively lower for impact loading as against to static loading (Bharatkumar *et al.* 2004).

From the literature, it is found that there is no systematic assessment of the response of UHPC panels subjected to low velocity. This absence provided the impetus for the work reported in this article, which forms the second part of the published work in Verma *et al.* (2016). In the first paper authors adopted smoothed particle hydrodynamics (SPH) method to predict the impact force and velocity. However it is known that mesh free methods and the SPH method are CPU time consuming. The idea in this paper is to restrict the use of SPH formulation and use finite element method (FEM) available in standard commercial packages for easier

*Corresponding author, Scientist

E-mail: prabhat@serc.res.in

^aScientist

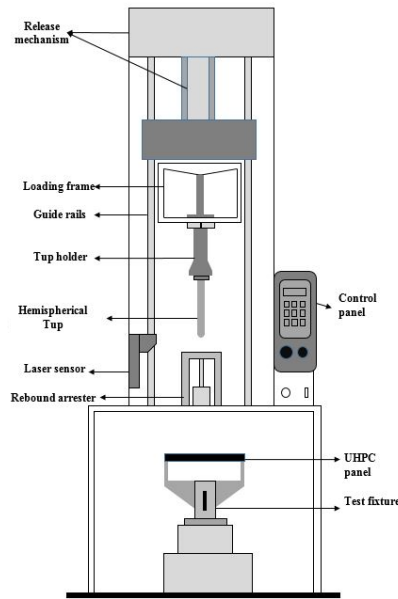


Fig. 1 Impact test set up

computation (Chuzel-Marmot *et al.* 2011, Thiyahuddin *et al.* 2012). The details of FEM modelling are presented in the subsequent sections. The theoretical modelling applied in this paper presents a more simple approach of predicting the impact force by application of energy based model compared to non - linear spring mass model used in the first paper. Authors also suggest an empirical relation for prediction of impact load using nonlinear multi-gene genetic programming.

2. Ultra high performance concrete

2.1 Mix design

The details of the mix design for UHPC are given in Table 1. The constituents of UHPC include 53 grade Portland cement of ASTM C 150/Type I, densified silica fume as per ASTM C 1240-97 with specific gravity of 2.2, quartz powder having particle size range of 5-25 μm and specific gravity 2.61, fine aggregate/standard sand as per Indian Standard 650 1991 and sizes as grade I (2-1 mm) and

Table 1 Mix proportion of UHPC

Cement	Silica fume	Quartz powder	Fine aggregates	Water	SP
kg/m ³	kg/m ³	kg/m ³	kg/m ³	l/m ³	l/m ³
788	197	315	866.8	173	14.77

grade III (0.5 mm - 0.09 mm) with a specific gravity of 2.65, straight brass coated micro steel fibers of 13 mm length and 0.16 mm diameter, high-range water-reducer and ordinary tap water. Three mixes known as R1, R2 and R3 are considered for the study. R1, R2 mixes have 2.5% and 2% volume of micro steel fibers while R3 have no micro steel fibers and is termed as plain UHPC. The mix used in the present study is based on earlier studies by authors using concepts of optimised particle packing (Ambily *et al.* 2015), proper curing techniques (Prem *et al.* 2013) and obtained mechanical properties using different micro steel fibers (Prem *et al.* 2015a).

2.2 Testing

Planetary mixer machine (300 kg capacity) is used to cast UHPC. The impact tests are carried out on UHPC concrete panels of size 350 mm×350 mm with thicknesses of 10 mm and 15 mm for mix R1, R2 and R3. The testing is performed by instrumented drop-weight impact testing machine Instron CEAST 9350. The impactor is a hemispherical tup having a nominal diameter of 10 mm. The nominal mass of the tup and tup holder is 1.11 and 4.3 kg, respectively. Therefore, the total mass impacting the UHPC panel is 5.41 kg. The impact tests are carried out at three energy levels of 10, 15 and 20 J. The height of the impactor is automatically adjusted based on the energy level. The schematics of the test setup is shown in Fig. 1. A single impact load is applied at the center of the panel. The panels are simply supported on two opposite edges. The impact force and velocity time histories of the center of the panel are recorded for 10 ms using a dynamic data logger at a sampling frequency of 20 kHz.

3. Impact behaviour of UHPC

The impact response of the tested panels for R2 mix

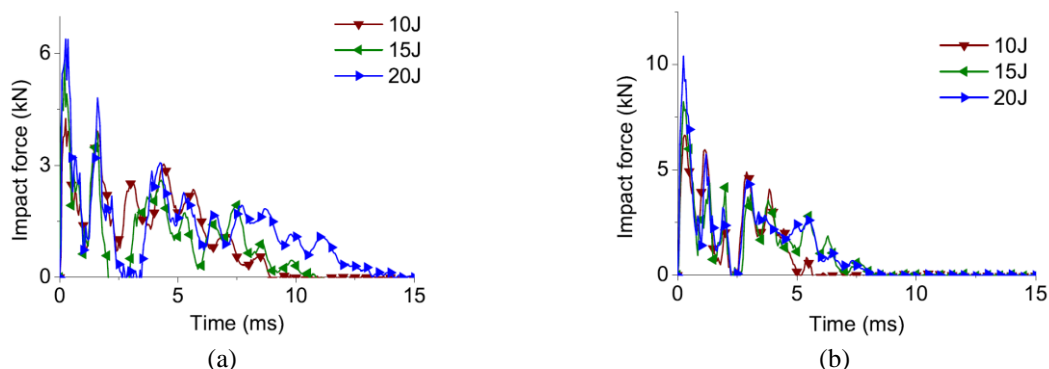


Fig. 2 Impact force time history for UHPC panels with R2 mix - (a) thickness - 10 mm (b) thickness - 15 mm

under 10, 15 and 20 J are presented in Fig. 2 (Verma *et al.* 2016). In general, it is found that R3 panels, have brittle failure, for both thickness of 10 mm and 15 mm, while subjected to energy level of 10 and 15 J. But the failure of plain UHPC (R3) is sudden when subjected to 20 J. The tested panel broke into several pieces and no data could be recorded for the same. From the experimental results it is interesting to see that, the peak load of R1 and R2 are almost same when tested in similar condition of impact energy and thickness of panel. Generally, the increase in fiber volume leads to increase in static performance (Maca *et al.* 2013), but here it did not enhance the performance under dynamic loading, which may be due to the increased inter-facial bond causing fracture of fibers instead of fiber pullout (Bindiganavile and Banthia 2001). Similar observations are also seen in earlier published research by authors on hybrid fiber reinforced concrete (Bharatkumar *et al.* 2004). The variation of the impact force against time is sinusoidal in nature. Low- velocity impact system can be idealized as a single or two degree of freedom system the free vibration response of which is sinusoidal in nature (Shivakumar *et al.* 1983). The amplitude and velocity are decreasing with time as the kinetic energy generated by impactor is dissipated in the form of plastic deformation and cracking. The damage in terms of panel deformation, integrity, cracks and cracks width reduced in the order of $R1 < R2 < R3$. As expected the failure mode of all the panels

is flexural as the thickness of the panel is very small compared to the other dimension and hence shear is not significant. For lower values of energy, only minor cracks are observed. With the increase in fiber volume post cracking resistance is improved and higher impulse energy is obtained. However from the studies 2% fiber volume with thickness of 15 mm panel is suggested for UHPC panels for application against low velocity impact. The reason being that the difference in mechanical strength and impact strength don't increase significantly when the volume of fiber is increased from 2% to 2.5%.

4. Impact test simulation

The simulation of the low velocity impact on UHPC is carried out by creating a model based on finite element method (FEM) in Abaqus/CAE. The results obtained from the model are then compared with those obtained from the experiments.

4.1 Geometry and boundary conditions

As the loading and geometry of panel are symmetrical, only a quarter part of the impactor and UHPC panel are modelled in the analysis. Symmetrical boundary conditions are applied on remaining sides of the panel as shown in Fig.

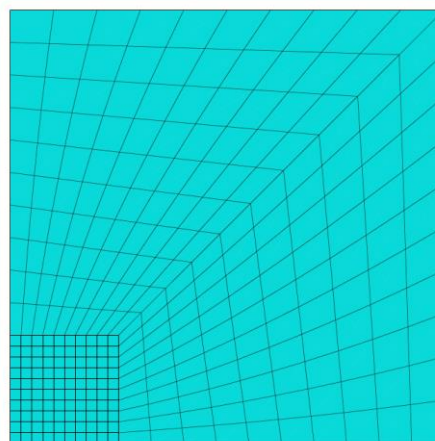
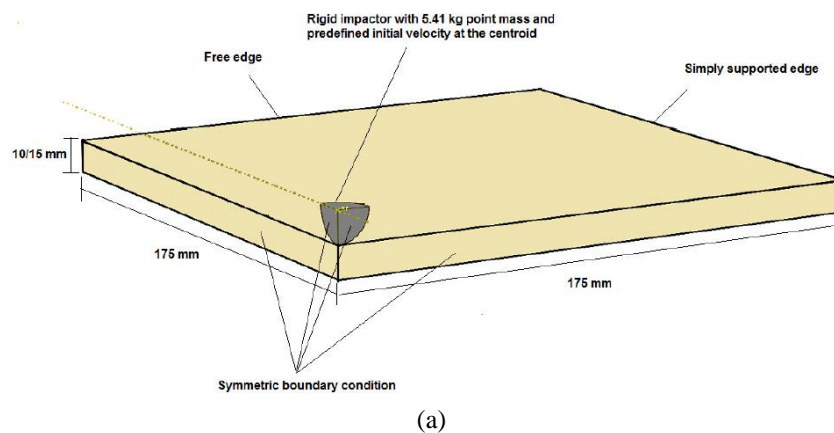


Fig. 3 Finite element model - (a) geometry, (b) mesh

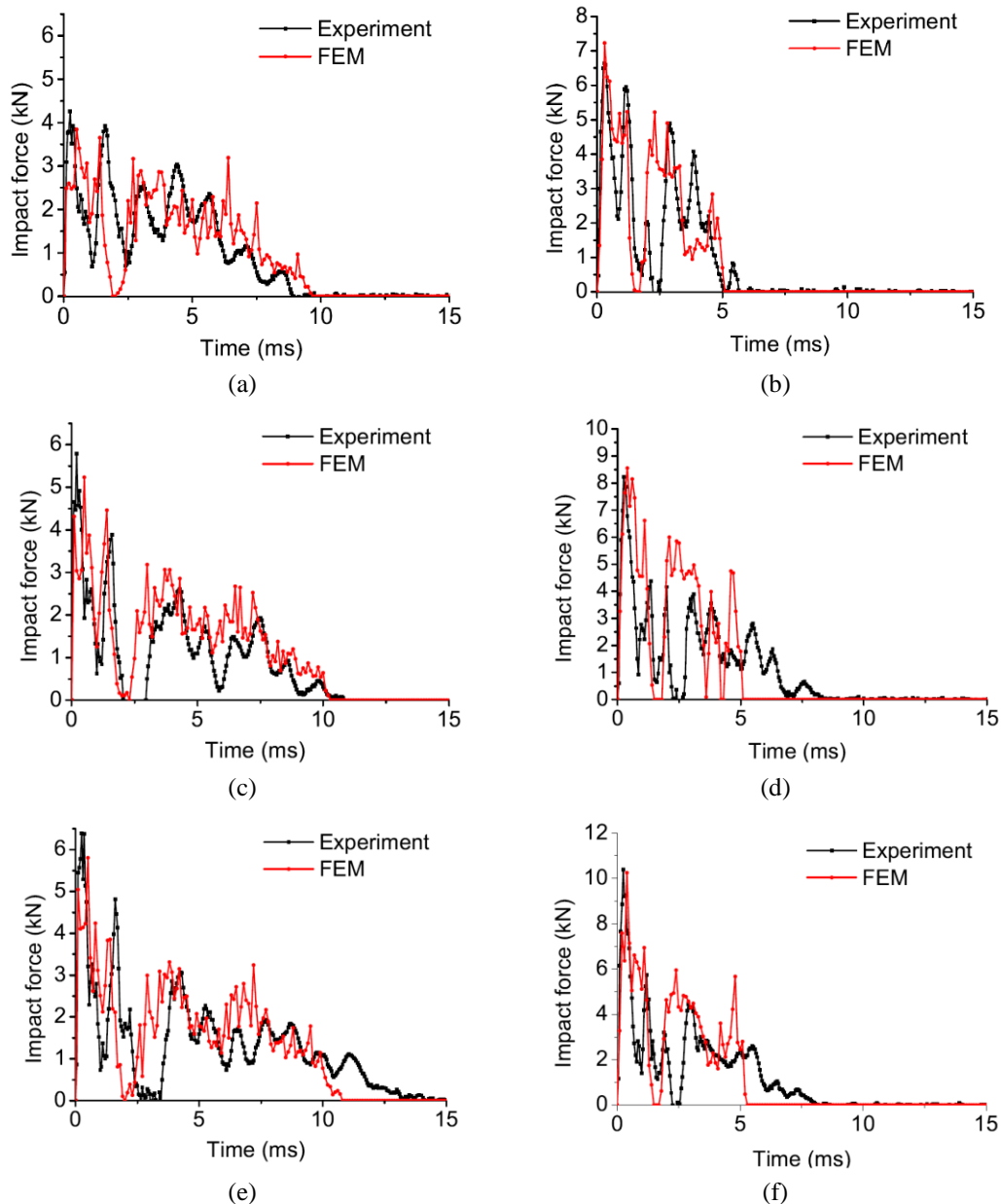


Fig. 4 Impact force time history of UHPC panels (a) thickness - 10 mm, energy - 10 J, (b) thickness - 15 mm, energy - 10 J, (c) thickness - 10 mm, energy - 15 J, (d) thickness - 15 mm, energy - 15 J, (e) thickness - 10 mm, energy - 20 J, (f) thickness - 15 mm, energy - 20 J

3. The steel impactor is modelled as a rigid body and a point mass corresponding to one-fourth mass of the impactor is located at the centroid of the impactor. The motion of the impactor is allowed only to move in the direction perpendicular to the plane of the panel. The normal hard contact is assumed between the impactor and the panel. Friction is not considered in the simulation. Edge biased structured mesh is used for UHPC panel (Fig. 3(b)). Coarser mesh is provided near the point of impact. Explicit dynamic analysis with 0.02s as time period and automatic time increment is used in FE simulation. The panel is discretized with the three dimensional linear reduced integration 8-node linear brick element (C3D8R) with hourglass control.

4.2 Modelling approach

The concrete damage plasticity (CDP) model is primarily employed to model the constitutive behavior of UHPC in this study. The model assumes isotropic damage elasticity combined with isotropic tensile and compressive plasticity to represent the inelastic behavior of concrete. Formation of tensile micro cracks is represented macroscopically with a softening stress-strain relationship (or stress-fracture energy relationship) and its compressive plastic response is represented by stress hardening followed by strain softening behaviour. To define a CDP model, a set of material parameters regarding compression hardening, tension stiffening, and other specific parameters should be

supplied in addition to density and elastic modulus based on the experimental testing results. The density of the mix is 2.56 kg/m^3 . The UHPC behaviour in compression is defined using stress and the inelastic strain values derived from the stress-strain curve obtained from the experiments. In the model it is assumed that the cracking in the concrete causes elastic modulus degradation, which is due to plastic straining in tension and compression of concrete. The isotropic damage of the material is given by Cauchy stress tensor (σ), where

$$\sigma = (1 - d) D_0^{e1} (\varepsilon - \varepsilon^{pl}) = D^{e1} (\varepsilon - \varepsilon^{pl}) d \quad (1)$$

and d is the scalar stiffness degradation variable, ε is the strain tensor, ε^{pl} is the plastic strain, D_0^{e1} is the elastic stiffness of the material, while $D^{e1} = (1 - d) D_0^{e1}$ is the degraded elastic stiffness tensor. The effective stress tensor is given by Eq. (2).

$$\bar{\sigma} = D_0^{e1} (\varepsilon - \varepsilon^{pl}) \quad (2)$$

The scalar degradation variable (d) is the function of the effective stress tensor ($\bar{\sigma}$) and hardening softening variable ($\bar{\varepsilon}^{pl}$). The stiffness degradation is initially isotropic and defined by degradation variable d_c in compression and d_t in tension. Hence, finally, the Cauchy stress tensor is related to effective stress tensor $\bar{\sigma}$ through the scalar degradation parameter $(1 - d)$ as

$$\sigma = (1 - d) \bar{\sigma} \quad (3)$$

The damage in tension and compression are characterized independently by two hardening softening variables as $\bar{\varepsilon}_t^{pl}$ and $\bar{\varepsilon}_c^{pl}$, which are referred as equivalent plastic strains in tension and compression, respectively. The evolution of this variables are given as follows

$$\bar{\varepsilon}^{pl} = \begin{bmatrix} \bar{\varepsilon}_t^{pl} \\ \bar{\varepsilon}_c^{pl} \end{bmatrix} \quad (4)$$

$$\dot{\bar{\varepsilon}}^{pl} = h(\bar{\sigma}, \bar{\varepsilon}^{pl}) \dot{\varepsilon}^{pl} \quad (5)$$

These variables control the evolution of the yield surface and degradation of elastic stiffness (Jankowiak and Lodygowski 2005).

The material properties of UHPC for R2 mix such as peak compressive stress (f_{ck}), tangent modulus (E_c), split tensile strength (f_{ctm}) and fracture energy (G_F) are given in Table 2 (Prem *et al.* 2015a). The post failure behaviour of UHPC in tension is carried by stress displacement response using fracture energy. Fracture energy approach is applied as it have been shown to obtain mesh insensitive results (Bazant and Planas 1997). The behaviour of UHPC in tension is defined using the fracture energy criteria to avoid the dependence of the results on the mesh size. The values for the tensile strength and fracture energy are set to the values obtained from the characterization of UHPC. The

other parameters required to fully describe a CDP model are dilation angle (α), flow potential eccentricity (e), ratio of initial equibiaxial compressive yield stress to initial uniaxial compressive yield stress ($\frac{f_{bo}}{f_{co}}$), ratio of the second stress invariant on the tensile meridian to that on the compressive meridian (K) and a viscosity parameter (μ) that defines viscoplastic regularization. The values for these parameters are 15, 0.1, 1.16, 2/3 and 0, respectively (Chen and Graybeal 2012).

4.3 Results and discussion

The simulation of the impact test is carried out by explicit dynamic analysis. The reaction force, position and velocity of the impactor are sampled at the rate of 20 kHz which are then compared with the results obtained from the experiments. The comparison of the impact force obtained from FEM with the experiments is shown in Fig. 4, for mix R2. The impactor velocity is obtained from the centroid of the rigid impactor. From the velocity response it is seen that there is initial deceleration due to high stiffness of UHPC panel in bending followed by rapid deceleration due to the dissipation of the kinetic energy of impactor in the form of plastic dissipation. A constant velocity plateau is observed due to rebound and separation of the impactor from the UHPC panel. The above analysis demonstrate that the CDP-based finite element model is capable of predicting the impact capacity of UHPC panels with good accuracy.

5. Theoretical modelling

An energy based model is applied to predict the impact response of the UHPC panel. The panel is considered to be isotropic and only the linear elastic response is considered. The energy losses due to friction, material damping, damage and higher modes of vibration are also neglected. This model is based on the conservation of the energy. The impactor's kinetic energy is equated to the energies stored in contact, membrane, shear and bending deformation. The energy conservation of the system can be written as (Shivakumar *et al.* 1983)

$$\frac{1}{2} M_i v^2 = E_c + E_{bs} + E_m \quad (6)$$

where M_i is the mass of the impactor, v is the velocity of the impactor, E_c , E_{bs} , E_m are the energies stored due to contact, bending-shear and membrane deformations. The energy is expressed as the integral of the product of force and deformation.

$$E_c = \int_0^\alpha P_c d\alpha \quad (7a)$$

$$E_{bs} = \int_0^\omega P_{bs} d\omega \quad (7b)$$

$$E_m = \int_0^\omega P_m d\omega \quad (7c)$$

Table 2 Material Properties of UHPC

f_{ck}	E_c	f_{ctm}	G_F
170.3	40	22.6	14.32

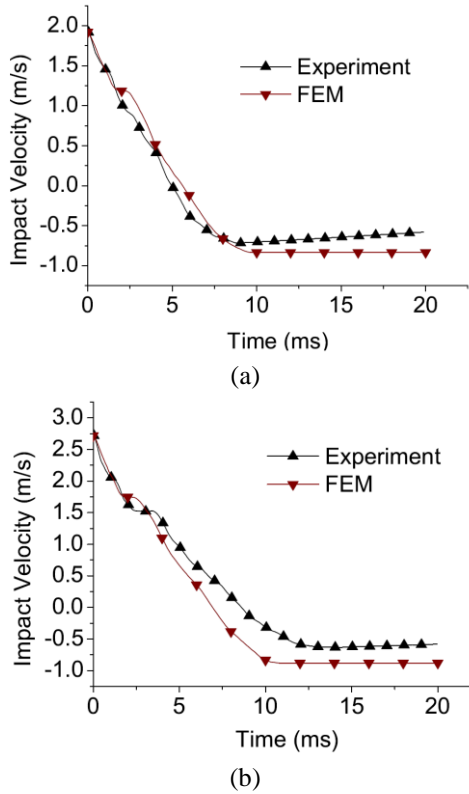


Fig. 5 Comparison of the impactor velocity (a) thickness - 10 mm, energy - 10 J, (b) thickness - 10 mm, energy - 20 J

where P_c, P_{bs}, P_m are the forces due to contact, bending-shear and membrane stresses, α is the contact deformation and ω is the panel deflection. The relationship between the impact force and the contact deformation is described by Hertz contact theory and is expressed as

$$P_c = K_c \alpha^3 \quad (8)$$

where K_c is the Hertzian contact stiffness. The forces due to bending - shear and membrane stresses is described by the following relation

$$P_{bs} = K_{bs} \omega \quad (9a)$$

$$P_m = K_m \omega^3 \quad (9b)$$

where K_{bs} is the effective stiffness in bending and shear, K_m is the membrane stiffness. The contact force is balanced by the forces due to bending-shear and membrane stresses.

$$P_c = P_{bs} + P_m = K_{bs} \omega + K_m \omega^3 \quad (10)$$

Using Eqs. (7)-(9) and further simplifications, the energy balance equation of the system can be written as (Shivakumar *et al.* 1983)

$$M_i v^2 = K_{bs} \omega^2 + \frac{K_m \omega^4}{2} + \frac{4}{5} \left[\frac{K_{bs} \omega + K_m \omega^3}{K_c^2} \right]^{\frac{1}{3}} \quad (11)$$

The above equation is then solved for w which is then substituted back in Eq. (10). In the present study shear and the membrane stresses are neglected. Therefore, effective bending shear stiffness is equal to the bending stiffness of

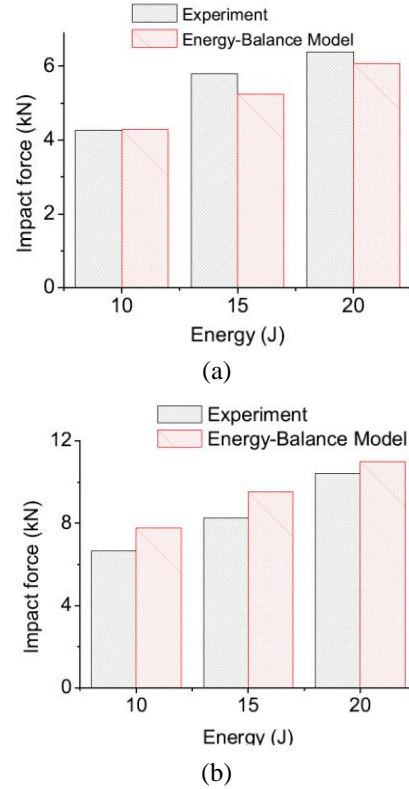


Fig. 6 Comparison of peak impact force obtained from energy-balance model with the experiments for different energy level - (a) thickness - 10 mm (b) thickness - 15 mm

the panel. The contact stiffness for an isotropic panel impacted by a spherical impactor is given by the following expression (Abrate 1991)

$$K_c = \frac{4}{3} \frac{\sqrt{R}}{\left(\frac{1 - \nu_i^2}{E_i} + \frac{1 - \nu_p^2}{E_p} \right)} \quad (12)$$

where R is the radius of the impactor, E is the Young's modulus and ν is the Poisson's ratio. The subscripts i and p corresponds to the impactor and panel. The generalized bending stiffness of an isotropic square panel simply supported on two opposite edges is given by

$$K_b = \frac{E_p h^3}{48 (1 - \nu_p^2)} \frac{\pi^4}{a^2} \quad (13)$$

where h is the thickness of the panel and a is the length of the panel. The peak impact force obtained from the experiments is compared with that obtained using energy-balance model in Fig. 6. The panels with mix R2 are selected for comparison. The results are found to be in good agreement with the experimental impact force. The impact force predicted by the energy balance model for 10 mm panel are found to be lower than that of the experiments.

The membrane stiffness, which is neglected, may have contributed to the impact force in the experiments. In case of 15 mm panels, the impact force obtained from the energy balance model are found to be on the higher side when compared to that obtained from the experiments. The

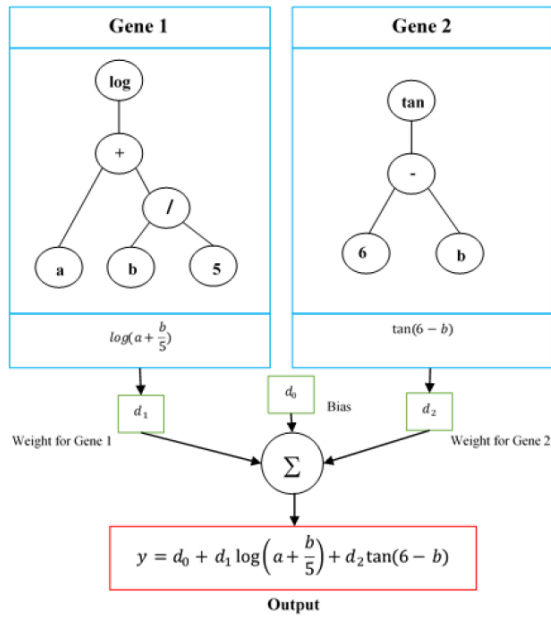


Fig. 7 MGGP model

bending stiffness of the 15 mm thick panel is over predicted due to the linear elastic behaviour assumption of UHPC panels.

6. Empirical relation

In order to arrive at an empirical relation for the impact load, nonlinear multi-gene genetic programming (MGGP) is used. MGGP is a form of symbolic regression carried out using Genetic Programming (GP). In MGGP, the initial population consists of the random generated GP trees. A mathematical expression is coded in each of the GP tree (Fig. 7).

$$P_c = 0.92p + 0.13hp + 0.14hv + 0.016pE - 0.26p^2 - 0.2 \quad (14)$$

The tree here is analogous to a gene. The tree is then evolved by the evolution process similar to that of GP.

Unlike traditional GP, the output of the MGGP model is the weighted linear combination of the output obtained from a number of GP trees. The output of MGGP can be viewed as the linear combination of the lower order nonlinear transformations of the input variables. More details can be found in (Searson *et al.* 2010, Gandomi and Alavi 2012, Searson 2014). The summary of the parameters used in MGGP are given in Table 3.

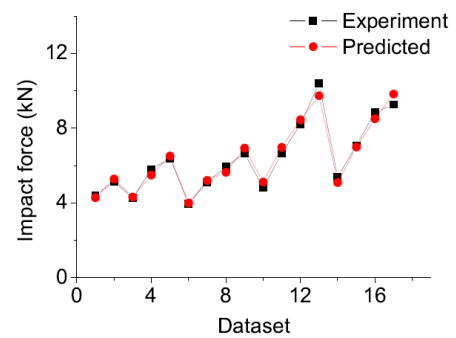
The peak impact force is assumed to be a function of thickness of the UHPC panel (h), percentage of fibers in the UHPC mix (p), energy of the impactor (E) and the initial velocity of the impactor (v). The dataset used for the development of empirical relation is given in Table 4.

6.1 Results and discussion

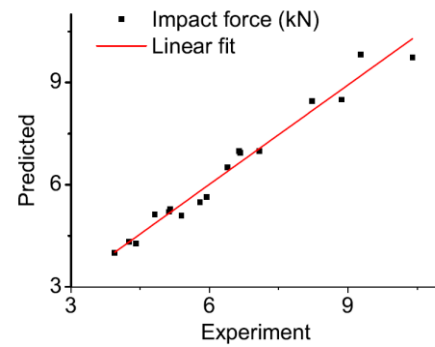
The relationship obtained from the empirical modelling

Table 3 Model parameters used in MGGP

Parameter	Value
Loss function	$\times, -, +$, square, tanh, sin, cos, exp
Population size	100
Number of generation	100
Maximum number of genes	5
Maximum tree depth	2
Tournament size	2
Elitism	0.02
Crossover events	0.85
Mutation events	0.1
Direct reproduction	0.05
Ephemeral random constants	[-10,10]



(a)



(b)

Fig. 8 Comparison of peak impact force obtained from empirical model with those obtained from experiments - (a) variation of impact force, (b) Linear fit ($R^2=0.97$)

is given by the following equation: The values of the impact force predicted are found to be in good agreement with the experimental values. The coefficient of correlation is found to be 0.97. In the present study, the generalization of the results based on the empirical equation may give only an approximate indication, as the domain of the data set is small. Nevertheless, it demonstrates that the technique could be used in the future studies to arrive at an empirical relation spanning over a larger domain.

7. Comparison of models

The energy based model and finite element method and

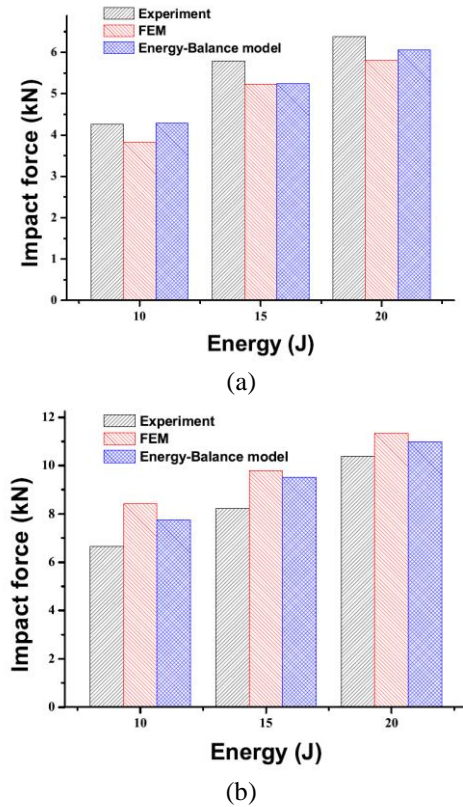


Fig. 9 Comparison of impact force predicted by different models

allow prediction of impact response of UHPC panel under different impact scenarios without conducting experiments. The impact force obtained using FEM simulations and developed energy model is shown in Fig. 9. The comparisons are done for 10 mm thick panel of R2 mix. From the comparison, it is found that both the models predict the peak impact load satisfactorily.

8. Conclusions

A numerical and theoretical procedure for modelling of low-velocity impact on UHPC panels was presented in this paper. The impact behaviour of UHPC panels was numerically simulated using finite element method (FEM). Concrete damage plasticity model was used to represent the behaviour of UHPC in tension and compression. Explicit dynamic analysis was carried out for three different energy levels of impactor and two different thickness of UHPC panels. The impact response obtained from the FE simulations was found to be in good agreement with experimental observations. A theoretical energy balance model based on the principle of conservation of total energy was also presented. The peak impact force predicted by energy balance model satisfactorily match with the experiments. In the end, an empirical relation for predicting the peak impact load was presented based on nonlinear multigene genetic programming. The values of the peak load obtained from the empirical relation were found to corroborate well with the experimental results.

Table 4 Dataset used for empirical modelling obtained from experiments

Sl. No	Thickness Mm	Fiber %	Energy J	Velocity m/s	Impact force kN
1	10	0	10	1.92	4.403
2	10	0	15	2.35	5.148
3	10	2	10	1.92	4.261
4	10	2	15	2.35	5.793
5	10	2	20	2.72	6.388
6	10	2.5	10	1.92	3.946
7	10	2.5	15	2.35	5.121
8	15	0	10	1.92	5.943
9	15	0	15	2.35	6.668
10	15	2	5	1.36	4.814
11	15	2	10	1.92	6.641
12	15	2	15	2.35	8.227
13	15	2	20	2.72	10.4
14	15	2.5	5	1.36	5.39
15	15	2.5	10	1.92	7.079
16	15	2.5	15	2.35	8.86
17	15	2.5	20	2.72	9.271

Acknowledgements

The authors would like to express their gratitude to Mr. Amar Prakash and Ms. Thirumalai Selvi of Shock and Vibration Group and technical support from the staff of Advanced Materials Laboratory for their help during the testing. Authors would like to extend their gratitude to the anonymous reviewer whose valuable comments have helped to improve the quality of the manuscript.

References

- Abrate, S. (1991), "Impact on laminated composite materials", *Appl. Mech. Rev.*, **44**(4), 155-90.
- Ambily, P., Umarani, C., Ravisankar, K., Prem, P.R., Bharatkumar, B. and Iyer, N.R. (2015), "Studies on ultra high performance concrete incorporating copper slag as fine aggregate", *Constr. Build. Mater.*, **77**, 233-240.
- Bazant, Z.P. and Planas, J. (1997), *Fracture and Size Effect in Concrete and Other Quasi Brittle Materials*, Volume 16, CRC Press.
- Bharatkumar, B., Shah, S., Weiss, J., Kovler, K., Marchand, J. and Mindess, S. (2004), "Impact resistance of hybrid fiber reinforced mortar", *International RILEM Symposium on Concrete Science and Engineering: A Tribute to Arnon Bentur*, RILEM Publications SARL.
- Bindiganavile, V. and Banthia, N. (2001), "Polymer and steel fiber-reinforced cementitious composites under impact loading? Part 2: flexural toughness", *ACI Mater. J.*, **98**(1), 17-24.
- Chen, L. and Graybeal, B.A. (2012), "Modeling structural performance of ultrahigh performance concrete I-girders", *J. Bridge Eng.*, **17**(5), 754-764.
- Chuzel-Marmot, Y., Ortiz, R. and Combescure, A. (2011), "Three dimensional SPH - FEM gluing for simulation of fast impacts on concrete slabs", *Comput. Struct.*, **89**(23), 2484-2494.
- Farnam, Y., Mohammadi, S. and Shekarchi, M. (2010), "Experimental and numerical investigations of low velocity

- impact behavior of high-performance fiber-reinforced cement based composite”, *Int. J. Impact Eng.*, **37**(2), 220-229.
- Gandomi, A.H. and Alavi, A.H. (2012), “A new multi-gene genetic programming approach to nonlinear system modeling. Part I: materials and structural engineering problems”, *Neur. Comput. Appl.*, **21**(1), 171-187.
- Habel, K. and Gauvreau, P. (2008), “Response of ultra-high performance fiber reinforced concrete (UHPRFC) to impact and static loading”, *Cement Concrete Compos.*, **30**(10), 938-946.
- Jankowiak, T. and Lodygowski, T. (2005), “Identification of parameters of concrete damage plasticity constitutive model”, *Found. Civil Environ. Eng.*, **6**(1), 53-69.
- Maca, P., Sovjak, R. and Konvalinka, P. (2014), “Mix design of UHPRFC and its response to projectile impact”, *Int. J. Impact Eng.*, **63**, 158-163.
- Maca, P., Sovjak, R. and Vavrinik, T. (2013), “Experimental investigation of mechanical properties of UHPRFC”, *Procedia Eng.*, **65**, 14-19.
- Mechtcherine, V., Millon, O., Butler, M. and Thoma, K. (2011), “Mechanical behaviour of strain hardening cement-based composites under impact loading”, *Cement Concrete Compos.*, **33**(1), 1-11.
- Murthy, A.R., Karihaloo, B.L., Iyer, N.R. and Prasad, B.R. (2013), “Determination of size independent specific fracture energy of concrete mixes by two methods”, *Cement Concrete Res.*, **50**, 19-25.
- Murthy, A.R., Kumar, V.R., Gopinath, S., Prem, P.R., Iyer, N.R. and Balakrishnan, R. (2014), “Structural performance of precast and cast-in-situ ultra high strength concrete sandwich panel”, *Int. J. Comput. Mater. Continua*, **44**(1), 59-72.
- Naaman, A., Toledo Filho, R., Silva, F., Koenders, E. and Fairbairn, E. (2011), “Half a century of progress leading to ultra-high performance fiber reinforced concrete: part 1 overall review”, *Proceedings of the 2nd International RILEM Conference*, 17-26.
- Prem, P.R. and Murthy, A.R. (2016), “Acoustic emission and flexural behaviour of RC beams strengthened with UHPC overlay”, *Constr. Build. Mater.*, **123**, 481-492.
- Prem, P.R., Bharathkumar, B. and Nagesh, R.I. (2012), “Mechanical properties of ultra high performance concrete”, *World Acad. Sci. Eng. Technol.*, **68**, 1969-1978.
- Prem, P.R., Bharathkumar, B. and Iyer, N.R. (2013), “Influence of curing regimes on compressive strength of ultra high performance concrete”, *Sadhana*, **38**(6), 1421-1431.
- Prem, P.R., Murthy, A.R. and Bharatkumar, B.H. (2015a), “Influence of curing regime and steel fibres on the mechanical properties of UHPC”, *Mag. Concrete Res.*, **67**(18), 988-1002.
- Prem, P.R., Murthy, A.R., Ramesh, G., Bharatkumar, B. and Iyer, N.R. (2015b), “Flexural behaviour of damaged RC beams strengthened with ultra high performance concrete”, *Adv. Struct. Eng.*, 2057-2069.
- Rokugo, K., Kanda, T., Yokota, H. and Sakata, N. (2009), “Applications and recommendations of high performance fiber reinforced cement composites with multiple fine cracking (HPRFC) in Japan”, *Mater. Struct.*, **42**(9), 1197-1208.
- Schmidt, M. (2012), “Sustainable building with ultra-high-performance concrete (UHPC) coordinated research program in Germany”, *Proceedings of Hipermat 2012 3rd International Symposium on UHPC and Nanotechnology for High Performance Construction Materials*, Kassel University Press, Kassel.
- Schmidt, M. and Fehling, E. (2005), “Ultra-high-performance concrete: research, development and application in Europe”, *ACI Special Publication*, **228**, 51-78.
- Searson, D.P. (2014), “GPTIPS 2: an open-source software platform for symbolic data mining”, *arXiv preprint arXiv:1412.4690*.
- Searson, D.P., Leahy, D.E. and Willis, M.J. (2010), “GPTIPS: an open source genetic programming toolbox for multigene symbolic regression”, *Proceedings of the International Multi Conference of Engineers and Computer Scientists*, Volume 1, Citeseer.
- Shivakumar, K., Elber, W. and Illg, W. (1983), “Prediction of impact force and duration during low velocity impact on circular composite laminates”, *J. Appl. Mech.*, **52**(3), 674-680.
- Sohel, K.M.A., Richard, L., Alwis, W.A.M. and Paramasivam, P. (2003), “Experimental investigation of low-velocity impact characteristics of steel-concrete-steel sandwich beams”, *Steel Compos. Struct.*, **3**(4), 289-306.
- Sovjak, R., Vavrin k, T., Zatloukal, J., Maca, P., Micunek, T. and Frydryn, M. (2015), “Resistance of slim UHPRFC targets to projectile impact using in-service bullets”, *Int. J. Impact Eng.*, **76**, 166-177.
- Tai, Y.S. and Wang, I.T. (2011), “Elucidating the mechanical behavior of ultra-high-strength concrete under repeated impact loading”, *Struct. Eng. Mech.*, **37**(1), 1-15.
- Thiyahuddin, I., Gu, Y., Thambiratnam, D. and Gudimetla, P. (2012), “Impact & energy absorption of road safety barriers by coupled SPH/FEM”, *Int. J. Protect. Struct.*, **3**(3), 257-273.
- Verma, M., Prem, P.R., Rajasankar, J. and Bharatkumar, B. (2016), “On low-energy impact response of ultra-high performance concrete (UHPC) panels”, *Mater. Des.*, **92**, 853-865.
- Wille, K., Naaman, A.E. and Parra-Montesinos, G.J. (2011), “Ultra-high performance concrete with compressive strength exceeding 150 MPa (22 ksi): A simpler way”, *ACI Mater. J.*, **108**(1), 34-46.
- Xu, J., Wu, C., Xiang, H., Su, Y., Li, Z.X., Fang, Q., Hao, H., Liu, Z., Zhang, Y. and Li, J. (2016), “Behaviour of ultra high performance fibre reinforced concrete columns subjected to blast loading”, *Eng. Struct.*, **118**, 97-107.
- Yoo, D.Y., Banthia, N., Kim, S.W. and Yoon, Y.S. (2015), “Response of ultra-high-performance fiber reinforced concrete beams with continuous steel reinforcement subjected to low-velocity impact loading”, *Compos. Struct.*, **126**, 233-245.
- Yu, R., Spiesz, P. and Brouwers, H. (2014), “Static properties and impact resistance of a green Ultra- High Performance Hybrid Fibre Reinforced Concrete (UHPRFC): experiments and modelling”, *Constr. Build. Mater.*, **68**, 158-171.
- Zhang, X., Ruiz, G. and Yu, R.C. (2010), “A new drop-weight impact machine for studying fracture processes in structural concrete”, *Strain*, **46**(3), 252-257.

CC